

On Path Length Estimation for Wireless Capsule Endoscopy

Anders Bjørnevik

Dept. of Research and Development
Kongsberg Seatex
Trondheim, Norway
anderssb@gmail.com

Pål Anders Floor

Dept. of Computer Science
NTNU
Gjøvik, Norway
paal.anders.floor@ntnu.no

Ilangko Balasingham

Dept. of Electronic Systems
NTNU
Trondheim, Norway
ilangkob@iet.ntnu.no

Intervention Center, Oslo University Hospital
Institute of Clinical Medicine, University of Oslo
Oslo, Norway
ilangko.balasingham@medisin.uio.no

Abstract—Wireless capsule endoscopy (WCE) is a non-invasive technology used for inspection of the gastrointestinal tract. Localization of the capsule is a vital part of the system enabling physicians to identify the position of anomalies. Due to intestinal motility, the positions of the intestines will change significantly within the abdominal cavity over time. However, the distance from one position to another within the intestines changes much less. In this paper a method for calculating the pathlength travelled by a WCE is proposed. The method is based on Kalman- and particle filters and is simulated using a model that approximately replicates the movement through the small intestine. The travelled distance was estimated to an accuracy within a few millimeters.

Index Terms—Wireless capsule endoscopy, localization, tracking, distance estimation.

I. INTRODUCTION

Wireless capsule endoscopy (WCE) is an emerging technology for examination of the gastrointestinal (GI) system. The patient is examined by swallowing a capsule containing a small video camera. The capsule follows the gastrointestinal system from the esophagus to the colon, locomoted by natural contractions in the intestines [1]. The physician examines the recorded images for abnormalities, enabling non-invasive diagnosis of diseases.

The video has to be accompanied by WCE position information so that the physician can return to the location of abnormalities at a later stage. The position can be estimated by localization methods based on for example microwave imaging [2], radio frequency (RF) signals [3], [4] or by including a permanent magnet in the capsule [5]. Accuracy can be improved by applying algorithms that track the movement of the WCE [4], [6].

Due to intestinal motility, the intestines are constantly moving [7]. This makes a fixed position of little relevance, since the position of the abnormality may have moved significantly at the time of treatment. A better way to approach this problem, is to use the distance travelled from a known point in the intestine, for instance the entry of the stomach [8]. This

distance is not as greatly affected by the intestinal movement as a fixed position, and is therefore of greater value to the physician.

In this paper a method for estimating the distance traveled by a WCE is proposed. The proposed scheme computes the pathlength traveled by the WCE from estimated positional information obtained from localization- and tracking algorithms. Several tracking algorithms are compared using a simulation model that approximately replicates the movement through the small intestine. We simplify, and illustrate the model in two dimensions. The same principles can be extended to three dimensions.

II. PROPOSED METHOD



Fig. 1. Block diagram for distance estimation.

The system can be characterized by three different modules, as shown in Fig. 1. The tracking system receives (2D) position estimates, (\hat{x}_i, \hat{y}_i) , from the localization framework that refines the positions, $(\tilde{x}_i, \tilde{y}_i)$, and estimates the current velocity, \tilde{v}_i , both which are used to estimate the distance.

A set of measurements $\{\mathbf{z}^i\} i = 1, \dots, P$, is used to estimate the positions (\hat{x}_i, \hat{y}_i) . As mentioned in the introduction, there are many possible localization methods. Although localization is a crucial part, this paper is concerned with tracking and distance estimation. Generally, the more exact the localization is, the better the performance of of the distance estimation (see Fig. 4). The efforts [4], [9], [10] evaluated localization accuracy within realistic media like the human abdominal model derived in [11] and a model based on measurements on a living porcine subject in [12]. It is shown that accuracy in the cm range is plausible for RF-based localization [9] and

that accuracy in the mm range is plausible for magnetic-based localization [13].

A. Distance Estimation

The problem of estimating the distance, \hat{d} , the WCE has travelled between a set of two-dimensional positions, $\{p_i\}$ $i = 1, \dots, n$, can be solved by:

- 1) Integrating the velocity v between the points:

$$\hat{d} = \int_{p_1}^{p_n} v(t) dt \quad (1)$$

- 2) Summing the Euclidean distances between each position:

$$\hat{d} = \sum_{i=1}^{n-1} \sqrt{(x_{i+1} - x_i)^2 + (y_{i+1} - y_i)^2}. \quad (2)$$

As Eq. (2) is only dependent on the positions of the WCE, 2) is the simplest method to implement as the positions are already available. However, this solution alone is not suitable since the capsule may stop for periods of time, typically within bends in the intestine. Thus, small errors in the position estimates will accumulate to errors in the distance that cause the estimated length \hat{d} to be longer than the true length d . The capsule velocity is needed to reduce this problem. Due to power consumption, it is not preferable to have sensors measuring the WCE velocity. Therefore, the velocity has to be estimated from the observed positions. With prior information about the previous positions available, a Bayesian approach would be a reasonable choice for such an algorithm [14].

As both velocity and positions are applied, the relevant state vector, \mathbf{x} , is on the form

$$\mathbf{x} = [x \quad \dot{x} \quad y \quad \dot{y}]^T. \quad (3)$$

The problem of estimating the state \mathbf{x}_k at time instant k using Bayesian dynamic state estimation (BSE) is given as [15]

$$\mathbf{x}_k = g(\mathbf{x}_{k-1}, \mathbf{u}_{k-1}, \mathbf{w}_{k-1}), \quad (4)$$

$$\mathbf{z}_k = h(\mathbf{x}_k, \mathbf{n}_k), \quad (5)$$

where g is a function relating the previous state \mathbf{x}_{k-1} with \mathbf{x}_k and h is a function that relates \mathbf{x}_k with the measurements \mathbf{z}_k . \mathbf{u}_k denotes a vector of known *control inputs*, while \mathbf{w}_k and \mathbf{n}_k are process and measurement noise, respectively.

B. Movement Model and Data Sets

In order to evaluate tracking algorithms, a model describing the functions g and h in (4) have to be found. The problem of modelling the movement of a WCE in the intestines was considered in [4]: The capsule movement is governed by the stress and strain cycle of the intestine, which can be considered constant under normal conditions. The main factors determining the speed is the diameter of the capsule (which is constant) and the intestines. The inner diameter of the intestines was found to change for different parts of the intestine in [16], causing small changes in velocity. As in [4], we simplify and assume that the intestines consists of L tubes

of different diameters, implying that we have L speed modes. Then, at time step k , the capsule speed can be approximated to follow the Gaussian mixture distribution [4]

$$v_k \approx \sum_{n=-L}^L p(n) \mathcal{N}(v_k | \mu_n, q_n), \quad (6)$$

where $\mathcal{N}(v_k | \mu_n, q_n)$ is a Gaussian pdf with mean μ_n , covariance q_n , and probability $p(n)$. At the end of each tube the capsule stops for a moment due to bends in the intestine.

The movement of a WCE in the intestines can therefore be approximated by the model in Fig. 2: The straight lines is where the capsule is moving close to constant speed and at the nodes the capsule is at rest.

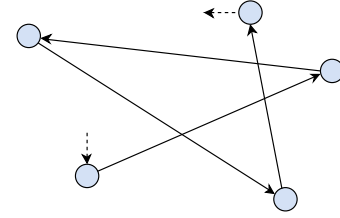


Fig. 2. A simplified motion model for the WCE movement. At the edges the WCE moves at approximately constant speed chosen from Eq. (6) and at the nodes it stops for a randomly chosen time interval.

The human model applied to generate relevant datasets is *HUGO* which is a complete anatomical three-dimensional model of the human body provided by the *Visible Human Project* [17]. The relevant datasets used for simulations were generated for the red dots shown in Figs. 3(a) and. 3(b), displaying two cross sections of the abdominal region of the HUGO model with a segment of about 30 cm of the small intestine included (the intestines are displayed as the black areas in the figures). The two cross-sections are located within the red rectangle shown in Fig. 3(c). For simplicity, the WCE was placed at the center of the intestine. In reality, more deviation from the midpoint is expected to occur. In the dataset generation, it was assumed that capsule positions were obtained every $T = 1$ seconds, which is in line with the existing WCE systems [18]. In every bend $< 135^\circ$ a random dwell time t_s was added to simulate the capsule stops.

C. Tracking Algorithms

For BSE, it is natural to use the *Kalman filter* (KF) [19]. However, since there are multiple speed modes as well as periods where the WCE is at rest one would assume that a *Multi model Kalman filter with variable noise level* (KF-VNL) [20], [21] would be a better choice. Further, the *particle filter* (PF) is a more general approach than the KF and applies to any state transition- and measurement model [22]. We will compare these three approaches, each of which is described in more detail in the following.

- i) **KF:** For the KF the state \mathbf{x}_k at time k is assumed to follow

$$\mathbf{x}_k = \mathbf{A}\mathbf{x}_{k-1} + \mathbf{B}\mathbf{u}_{k-1} + \mathbf{w}_{k-1}, \quad (7)$$

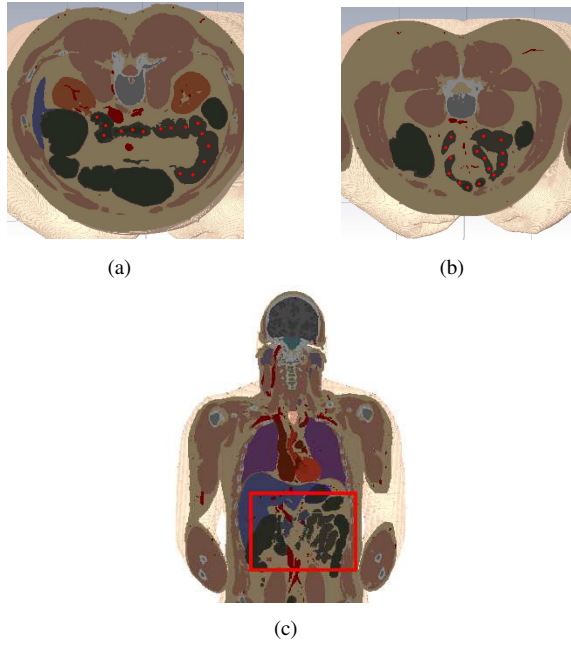


Fig. 3. Cross-sections of a human abdominal region. The red dots are points placed in the small intestine used as a reference when creating datasets for tracking: (a) Dataset 1. (b) Dataset 2. (c) Location of the two cross-sections within the HUGO model.

where the observation of \mathbf{x}_k is given as

$$\mathbf{z}_k = \mathbf{C}\mathbf{x}_k + \mathbf{n}_k. \quad (8)$$

\mathbf{w}_k and \mathbf{n}_k have distributions $p(w) \sim \mathcal{N}(0, \mathbf{Q})$ and $p(n) \sim \mathcal{N}(0, \mathbf{R})$ respectively. The covariance matrices \mathbf{Q} and \mathbf{R} are assumed constant. For constant velocity (\dot{x}, \dot{y}) with measurements of positions (x, y) and timestep T , the state transition matrix \mathbf{A} and the observation matrix \mathbf{C} are given by

$$\mathbf{A} = \begin{bmatrix} 1 & T & 0 & 0 \\ 0 & 1 & 0 & 0 \\ 0 & 0 & 1 & T \\ 0 & 0 & 0 & 1 \end{bmatrix}, \quad \mathbf{C} = \begin{bmatrix} 1 & 0 & 0 & 0 \\ 0 & 0 & 1 & 0 \end{bmatrix}. \quad (9)$$

The control input matrix \mathbf{B} was chosen as zero, with mismatch in the model compensated for by increased noise in the process noise covariance matrix \mathbf{Q} . The covariance matrix for observation noise was chosen as $\mathbf{R} = \text{diag}(\sigma_{r,x}^2, \sigma_{r,y}^2)$, where $\sigma_{r,x}^2$ and $\sigma_{r,y}^2$ are the variances of the measured noisy observations, while the covariance matrix $\mathbf{Q} = \text{diag}(0, \sigma_{q,x}^2, 0, \sigma_{q,y}^2)$ where $\sigma_{q,x}^2$ and $\sigma_{q,y}^2$ represent unmodelled accelerations when the capsule is moving. For more details on implementation of the KF see for example [4].

ii) KF-VNL: The KF-VNL operates with multiple observation noise covariance matrices, $\mathbf{Q}_1, \dots, \mathbf{Q}_n$, corresponding to different modes in the filter.

In this paper, a two-mode KF-VNL is considered with \mathbf{Q}_1 and \mathbf{Q}_2 , given by $\mathbf{Q}_1 = \text{diag}(0, \sigma_{q1,x}^2, 0, \sigma_{q1,y}^2)$ and $\mathbf{Q}_2 = \text{diag}(0, \sigma_{q2,x}^2, 0, \sigma_{q2,y}^2)$ respectively. The variances $\sigma_{q1,x}^2$ and $\sigma_{q1,y}^2$ represent unmodelled accelerations when the capsule is moving. $\sigma_{q2,x}^2$ and $\sigma_{q2,y}^2$ correspond to process noise that

compensates for the transition between the WCE moving and being stopped.

More details on how this 2-mode KF-VNL can be implemented is given in [21].

iii) PF: With a set of measurements $D_k = \{\mathbf{z}_i : i = 1, \dots, k\}$, the goal is to determine $p(\mathbf{x}_k | D_k)$ recursively: One can write [22]

$$p(\mathbf{x}_k | D_{k-1}) = \int p(\mathbf{x}_k | \mathbf{x}_{k-1}) p(\mathbf{x}_{k-1} | D_{k-1}) d\mathbf{x}_{k-1}. \quad (10)$$

When a new observation \mathbf{z}_k is available, then

$$p(\mathbf{x}_k | D_k) = \frac{p(\mathbf{z}_k | \mathbf{x}_k) p(\mathbf{x}_k | D_{k-1})}{p(\mathbf{z}_k | D_{k-1})}. \quad (11)$$

where the normalization $p(\mathbf{z}_k | D_{k-1})$ is as in (10) with \mathbf{x}_k replaced by \mathbf{z}_k and \mathbf{x}_{k-1} replaced by \mathbf{x}_k . Let $\{\mathbf{x}_{k-1}(i) : i = 1, \dots, N\}$ random samples from $p(\mathbf{x}_k | D_{k-1})$ be available. The PF approximates the relations in Eq. (10-11) through the two steps [22]:

Prediction: Pass each sample in the set through the system model to obtain

$$\mathbf{x}_k^*(i) = g(\mathbf{x}_{k-1}(i), \mathbf{w}_{k-1}(i)). \quad (12)$$

$\mathbf{w}_{k-1}(i)$ is drawn from the system noise pdf $p(\mathbf{w}_{k-1})$.

Update: When a new measurement \mathbf{z}_k is available, evaluate the likelihood of each prior sample and obtain the normalised weights

$$q_k(i) = \frac{p(\mathbf{z}_k | \mathbf{x}_k^*(i))}{\sum_{j=1}^N p(\mathbf{z}_k | \mathbf{x}_k^*(j))}. \quad (13)$$

The filtered posterior density is then

$$p(\mathbf{x}_k | D_k) \approx \sum_{i=1}^N q_k(i) \delta(\mathbf{x}_k - \mathbf{x}_k^*(i)), \quad (14)$$

where the approximation becomes equality as $N \rightarrow \infty$ [23].

The PF starts by initializing N particles $\mathbf{x}_0^1, \dots, \mathbf{x}_0^N$ according to $\mathcal{N}(\mathbf{x}_0, \Sigma)$, where \mathbf{x}_0 is the initial state provided to the filter and Σ are the variances of the initial particles. Using the constant velocity dynamic model with the state vector in Eq. (3), the state evolution in (12) becomes $\mathbf{x}_k^i = \mathbf{A}\mathbf{x}_{k-1}^i + \mathbf{n}$, where \mathbf{x}_k^i is particle number i representing one proposed state vector at time k . \mathbf{A} is as in (9) and $\mathbf{n} \sim \mathcal{N}(0, \Sigma)$.

Since the noise model is assumed to be Gaussian, we have

$$p(\mathbf{z}_k | \mathbf{x}_k(i)) = \frac{1}{\sqrt{(2\pi)^M |\det(\mathbf{R})|}} \exp\left(-\frac{1}{2}(\boldsymbol{\pi}_k^i)^T \mathbf{R}^{-1} \boldsymbol{\pi}_k^i\right), \quad (15)$$

where $\boldsymbol{\pi}_k^i = \mathbf{z}_k - \mathbf{x}_k(i)$ and \mathbf{z}_k has covariance \mathbf{R} . The reconstruction is then $\hat{\mathbf{x}}_k = \sum_{i=1}^N \mathbf{x}_k(i) p(\mathbf{z}_k | \mathbf{x}_k(i))$.

For the PF resampling process, the cumulative distribution of the particle weights were used in order to discard particles with negligible probability. In order to weight both the position and the velocity estimate during resampling, the observation vector was chosen as

$$\mathbf{z}_k = [x_k \quad y_k \quad \sqrt{(x_k - x_{k-1})^2 + (y_k - y_{k-1})^2} / T]^T. \quad (16)$$

TABLE I
PARAMETERS USED UNDER
SIMULATION [4].

Parameter	Value
\bar{v}	0.5 mm/s
σ_v	0.05 mm/s
t_s	5 min
σ_s	10 min

TABLE II
SETTINGS USED FOR KF AND PF.

Description	Value
Noise level	SNR = 25 dB
Simulations	$S = 100$
Number of particles	$N = 10000$
Initial particle noise	$\sigma_{N_0} = 1$

III. SIMULATIONS

For all simulations the velocity was chosen as $\mathcal{N}(\bar{v}, \sigma_v)$, with the stop time, t_s , modelled as $|\mathcal{N}(t_s, \sigma_s)|$ following the investigations done in [4]. Specific values are given in Tab. I. The chosen values for all tracking algorithms are summarized in Tab. II. Timesteps for the 2nd mode of the KF VNL was chosen as $r = 100$.

The following measures are applied in order to evaluate the algorithms:

- i) Signal-to-noise ratio (SNR) [24]

$$\text{SNR} = 10 \log_{10} \left(\frac{1}{N \sigma_r^2} \sum_{n=1}^N x_n \right) \quad (17)$$

where x is the relevant signal and σ_r^2 is the (observation) noise variance.

- ii) For the distance estimation problem, the mean difference in length over S simulations is computed as

$$\Delta = \frac{1}{S} \sum_{n=1}^S (\hat{d}_n - d), \quad (18)$$

where d is the true distance and \hat{d}_n is the distance estimate.

In order to obtain the best estimate of the path length, all filters were tuned for the minimum Δ . The system should ideally be optimized for the most relevant SNR. However, this value will change throughout the intestine as well as from person to person depending on the size of the torso. Here we chose to optimize the system for SNR = 25 dB as was used for the detailed simulations in [24]. Due to the variation in SNR it is of interest to compare the effect of the varying observation noise on the distance estimates. The result can be seen in Fig. 4, where SNR levels between 10-45 dB have been used. The resulting Δ for each SNR value was found from 100 Monte-carlo simulations. For dataset 1, the KF-VNL has the best performance for most of the SNR values. For dataset 2, the KF performs best for low SNR. The PF is most susceptible to low SNR for both datasets, but has the best performance at high SNR. Due to the filters being tuned for operation at 25 dB SNR, the full performance of the KF-VNL is not utilized at low SNR, as the increased noise causes problems in detecting the capsule maneuvers.

IV. DISCUSSION AND CONCLUSIONS

In this paper a method for estimating the pathlength traversed by a wireless capsule endoscope (WCE) traveling

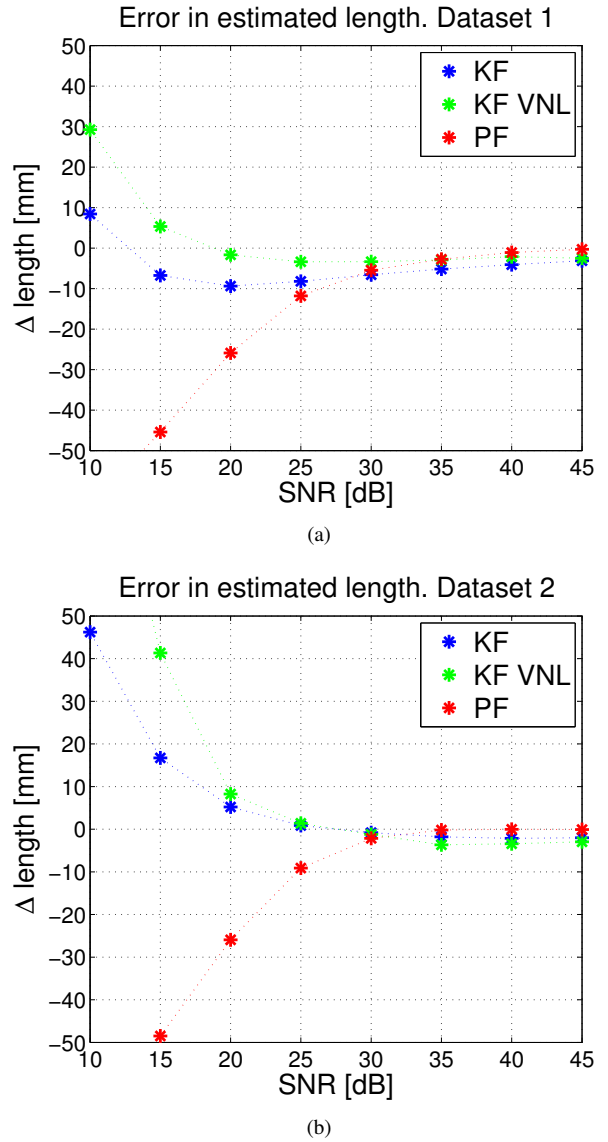


Fig. 4. Deviation from actual path length, Δ , for different SNR levels. (a) Dataset 1. (b) Dataset 2.

through the human gastrointestinal tract has been proposed. The method is built around known localization and tracking algorithms. Three tracking algorithms were tested: Kalman filter (KF), multi model KF with variable noise level (KF-VNL) and particle filter (PF). The distance is computed based on the output of the chosen tracking algorithm

The KF-VNL was found to have the most accurate distance estimation over the broadest range of position-to-observation signal-to-noise ratios (SNR), being within ± 3 mm above 25 dB SNR. However, if the SNR increases the PF becomes more accurate with an error approaching 0 mm. As the SNR drops below 15 dB, the KF outperforms the KF-VNL. The reason for this is probably that the KF-VNL was not tuned for SNR below 25 dB. The performance of the PF could be increased at low SNR with a larger amount of particles at the cost of

longer computation time.

For all tracking algorithms the performance increases as the observation noise is reduced. A high performance localization system combined with the tracking algorithms is expected to have a distance estimation accuracy in the order of millimeters.

In [25] a video-based distance estimation algorithm obtains an accuracy of 2.71 cm for a 500 cm long path with velocity within 0-4 mm/s. Comparing this to the result of ± 3 mm presented in Sec. III, it seems at first glance that our proposed scheme has a better performance for this specific setup. However, apart from being of different lengths, the datasets used for evaluation have significant differences: In [25], it is assumed that the capsule constantly changes velocity between 0-4 mm/s. The datasets we generated here have only minor deviations in the velocity when the capsule is moving, and has long periods when the capsule is at rest. It is unknown how well the algorithm in [25] performs for datasets that contain long periods with no capsule movement, and how our approach perform for a larger stretch of intestine. Further research is needed to conclude.

The results of this paper are entirely simulation based and meant to indicate a plausible accuracy for the proposed scheme. As a proof of concept it is important to evaluate the accuracy using real pillcams on several human test subjects of different sizes. This study will require a significant effort that should be pursued through future research.

REFERENCES

- [1] G. Ciuti, A. Menciassi, and P. Dario, "Capsule endoscopy: from current achievements to open challenges." *IEEE reviews in biomedical engineering*, vol. 4, pp. 59–72, Jan. 2011.
- [2] R. Chandra, A. J. Johansson, M. Gustafsson, and F. Tufvesson, "A microwave imaging-based technique to localize an in-body RF source for biomedical applications." *IEEE transactions on bio-medical engineering*, vol. 62, no. 5, pp. 1231–41, May 2015.
- [3] D. Fischer, R. Schreiber, D. Levi, and R. Eliakim, "Capsule endoscopy: the localization system." *Gastrointestinal endoscopy clinics of North America*, vol. 14, no. 1, pp. 25–31, Jan. 2004.
- [4] B. Moussakhani, "On Localization and Tracking for Wireless Capsule Endoscopy," Ph.D. dissertation, NTNU, 2013. [Online]. Available: <https://brage.bibsys.no/xmlui/handle/11250/2370705>
- [5] C. Hu, W. Yang, D. Chen, M. Q. H. Meng, and H. Dai, "An improved magnetic localization and orientation algorithm for wireless capsule endoscope." *Annual International Conference of the IEEE Engineering in Medicine and Biology Society. IEEE Engineering in Medicine and Biology Society. Annual Conference*, vol. 2008, pp. 2055–8, Jan. 2008.
- [6] G. Bao, K. Pahlavan, and L. Mi, "Hybrid Localization of Microrobotic Endoscopic Capsule Inside Small Intestine by Data Fusion of Vision and RF Sensors," *IEEE Sensors Journal*, vol. 15, no. 5, pp. 2669–2678, May 2015.
- [7] W. A. Kunze and J. B. Furness, "The enteric nervous system and regulation of intestinal motility." *Annual review of physiology*, vol. 61, pp. 117–42, Jan. 1999.
- [8] K. Pahlavan, G. Bao, Y. Ye, S. Makarov, U. Khan, P. Swar, D. Cave, A. Karellas, P. Krishnamurthy, and K. Sayrafian, "RF Localization for Wireless Video Capsule Endoscopy," *International Journal of Wireless Information Networks*, vol. 19, no. 4, pp. 326–340, Oct. 2012.
- [9] B. Moussakhani, J. Flåm, S. Støa, I. Balasingham, and T. Ramstad, "On localisation accuracy inside the human abdomen region," *IET Wireless Sensor Systems*, vol. 2, no. 1, p. 9, 2012.
- [10] A. Bjørnevik, *Localization and Tracking of Intestinal Paths for Wireless Capsule Endoscopy*. M.Sc. thesis, NTNU, 2015. [Online]. Available: <https://brage.bibsys.no/xmlui/handle/11250/2371524>
- [11] S. Stoa, R. Chavez-Santiago, and I. Balasingham, "An ultra wideband communication channel model for the human abdominal region," in *2010 IEEE Globecom Workshops*. IEEE, Dec. 2010, pp. 246–250.
- [12] P. A. Floor, R. Chavez-Santiago, S. Brovoll, O. Aardal, J. Bergsland, O.-J. Grymyr, P. S. Halvorsen, R. Palomar, D. Pletteimeier, S.-E. Hamran, T. Ramstad, and I. Balasingham, "In-Body to On-Body Ultra Wideband Propagation Model Derived from Measurements in Living Animals." *IEEE journal of biomedical and health informatics*, vol. PP, no. 99, p. 1, Apr. 2015.
- [13] B. Moussakhani, T. A. Ramstad, J. Flåm, and I. Balasingham, "On localizing a capsule endoscope using magnetic sensors," in *Engineering in Medicine and Biology Society (EMBC), 2012 34th Annual International Conference of the IEEE*. ACM, 2012, pp. 4058–4062.
- [14] S. M. Kay, *Fundamentals of Statistical Signal Processing: Practical algorithm development*. Prentice-Hall PTR, 2013.
- [15] G. Welch and G. Bishop, "An Introduction to the Kalman Filter," Nov. 2006. [Online]. Available: <http://dl.acm.org/citation.cfm?id=897831>
- [16] X. Wang and M. Q.-H. Meng, "An experimental study of resistant properties of the small intestine for an active capsule endoscope." *Proceedings of the Institution of Mechanical Engineers. Part H, Journal of engineering in medicine*, vol. 224, no. 1, pp. 107–18, Jan. 2010.
- [17] M. Ackerman, "The Visible Human Project," *Proceedings of the IEEE*, vol. 86, no. 3, pp. 504–511, Mar. 1998.
- [18] J. L. Toennies, G. Tortora, M. Simi, P. Valdastrì, and R. J. Webster, "Swallowable medical devices for diagnosis and surgery: the state of the art," *Proceedings of the Institution of Mechanical Engineers, Part C: Journal of Mechanical Engineering Science*, vol. 224, no. 7, pp. 1397–1414, Jan. 2010.
- [19] R. E. Kalman, "A New Approach to Linear Filtering and Prediction Problems," *Journal of Basic Engineering*, vol. 82, no. 1, p. 35, Mar. 1960.
- [20] V. Jilkov, "Survey of maneuvering target tracking. part v: multiple-model methods," *IEEE Transactions on Aerospace and Electronic Systems*, vol. 41, no. 4, pp. 1255–1321, Oct. 2005.
- [21] B. Moussakhani, R. Chavez-Santiago, and I. Balasingham, "Multi Model Tracking for Localization in Wireless Capsule Endoscope," in *2011 4th International Symposium on Applied Sciences in Biomedical and Communication Technologies (ISABEL 2011)*. ACM, 2011.
- [22] N. Gordon, D. Salmond, and A. Smith, "Novel approach to nonlinear/non-Gaussian Bayesian state estimation," *IEE Proceedings for Radar and Signal Processing*, vol. 140, no. 2, pp. 107–113, 1993.
- [23] M. Arulampalam, S. Maskell, N. Gordon, and T. Clapp, "A tutorial on particle filters for online nonlinear/non-Gaussian Bayesian tracking," *IEEE Transactions on Signal Processing*, vol. 50, no. 2, pp. 174–188, 2002.
- [24] Z. Xiahou and X. Zhang, "Adaptive Localization in Wireless Sensor Network through Bayesian Compressive Sensing," *International Journal of Distributed Sensor Networks*, 2015.
- [25] Guanqun Bao, Liang Mi, Yishuang Geng, Mingda Zhou, and K. Pahlavan, "A video-based speed estimation technique for localizing the wireless capsule endoscope inside gastrointestinal tract." in *Engineering in Medicine and Biology Society (EMBC), 2014 36th Annual International Conference of the IEEE*, Aug. 2014, pp. 5615–5618.